

# Solar Rotational Tomography of the Corona with Latest Instrumentation

A.M. Vasquez, F.A. Nuevo, R.A. Frazin, A. Burtovoi,  
P. Lamy, M. Romoli, E. Landi, H. Gilardy, F. Frassati,  
A. Bemporad, R. Susino, N. Sachdeva, W. Manchester IV

Instituto de Astronomía y Física del Espacio (IAFE), Buenos Aires–Argentina

Dipartimento di Fisica e Astronomia, Università degli Studi di Firenze (UniFi), Firenze–Italy

Laboratoire Atmosphères, Milieux et Observations Spatiales (LATMOS), CNRS & UVSQ, Guyancourt–France

Istituto Nazionale di Astrofisica (INAF), Osservatorio Astrofisico di Torino (OATo), Pino Torinese–Italy

Department of Climate and Space Sciences and Engineering (ClaSP), University of Michigan, Ann Arbor–USA



PUNCH 5 Science Meeting – June 21, 2024

# Outline

- **Solar rotational tomography (SRT)** uses sequences of coronal images to determine the 3D distribution of coronal physical parameters ( $N_e$ ,  $T_e$ , see [Poster](#)).
- WL images are a direct diagnostic of the coronal  $N_e$  along the LOS. SRT-WL allows determination of the 3D coronal  $N_e$ .
- The **SOLO/Metis** coronagraph records WL and Lyman- $\alpha$  images.
  - SRT can be used for reconstruction of  $N_e$  and Doppler-dimming term.
  - Its highly eccentric orbit implies a varying range of observed heights.
  - The synoptic Metis images can be used for tomography during most of its planned orbit [Vasquez et al. \(2022\)](#).
- The **MLSO/UCoMP** coronagraph records images in optical emission lines.
  - SRT can be applied for reconstruction of their 3D coronal emissivity.
  - This can be used for 3D diagnostics, such as line-ratio  $N_e$ .
- Here we show first results of SRT applied to both Metis and UCoMP data.

# A Superior Conjunction of SOLO and SOHO

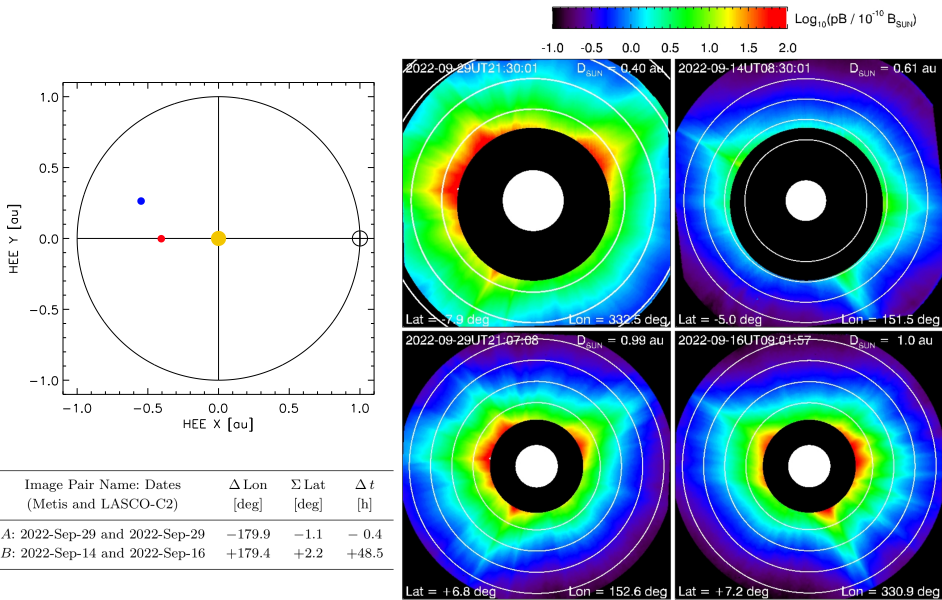
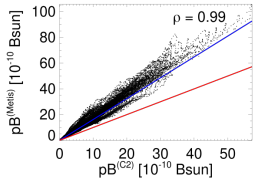
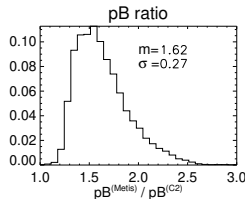
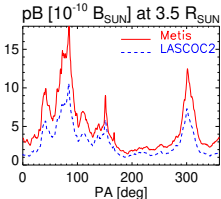


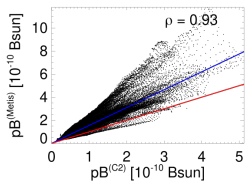
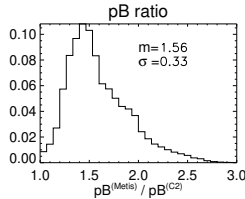
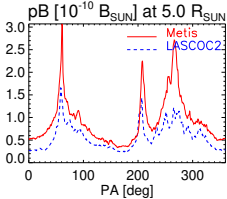
Image Pair Name: Dates (Metis and LASCO-C2)	$\Delta \text{Lon}$ [deg]	$\Sigma \text{Lat}$ [deg]	$\Delta t$ [h]
A: 2022-Sep-29 and 2022-Sep-29	-179.9	-1.1	- 0.4
B: 2022-Sep-14 and 2022-Sep-16	+179.4	+2.2	+48.5

# Comparison of Metis and C2 Images

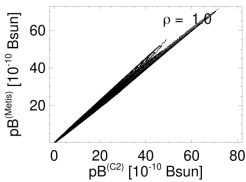
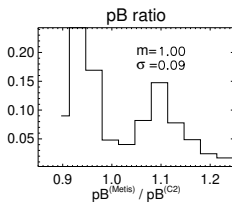
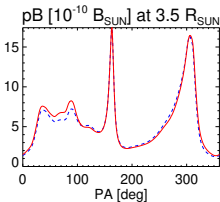
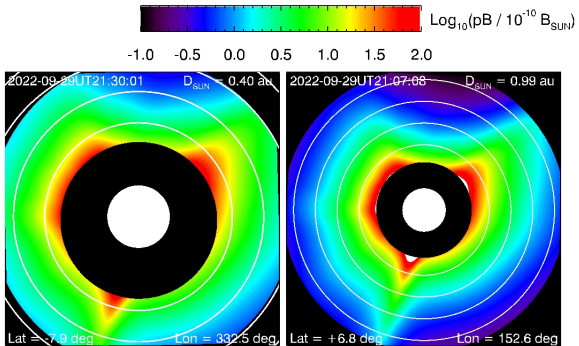
Superior Conjunction: Median  $\left( pB^{(\text{Metis})} / pB^{(\text{C2})} \right) \approx 1.62$



Two Days Apart: Median  $\left( pB^{(\text{Metis})} / pB^{(\text{C2})} \right) \approx 1.56$



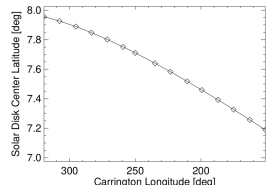
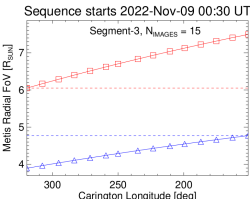
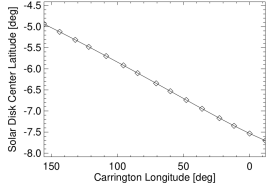
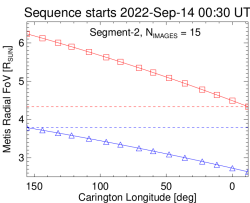
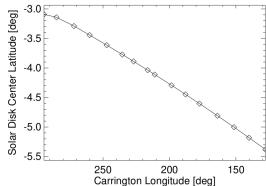
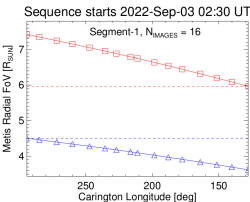
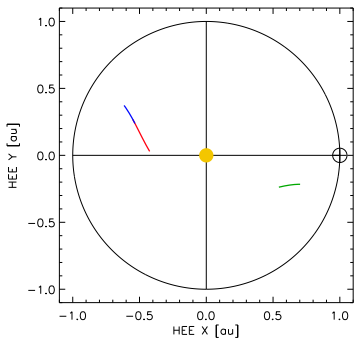
# Synthetic Images from 3D-MHD Simulation



# SRT with Metis WL Images

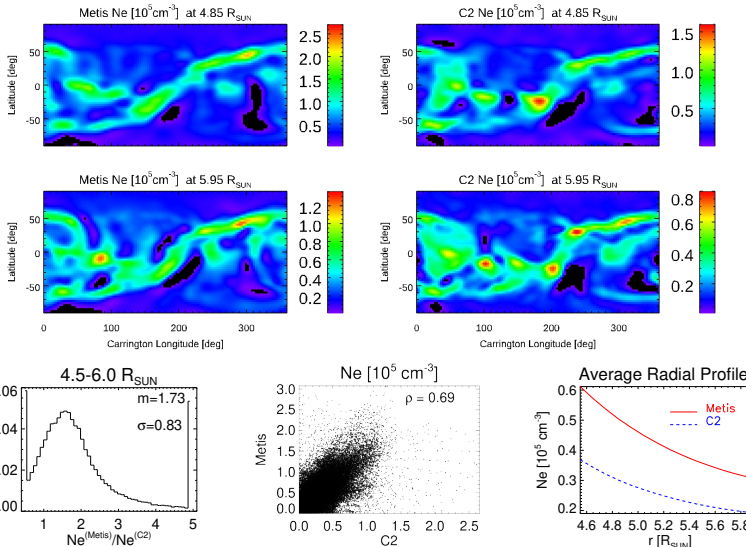
- SRT has been applied to data from both ground-based (e.g. MLSO/KCOR) and space-borne (SOHO/C2) instruments, from  $\approx 1$  AU (nearly) circular orbits.
- C2 images (1996-present) with [Lamy et al. \(2020\)](#) best-to-date calibration are available at the C2 Legacy Archive (<http://idoc-lasco.ias.u-psud.fr>).
- In the case of Metis, the high eccentricity of the SOLO orbit implies that the FoV of the images is a function of the orbital position.
- Orbital analysis of SOLO/Metis shows that its synoptic program allows for continuous SRT reconstruction of the coronal  $N_e$  ([Vasquez et al. 2022](#)).
- Here we show first tomographic reconstructions carried out with Metis images, and their comparison with C2 tomography.

# Three SOLO Orbital Segments During 2022



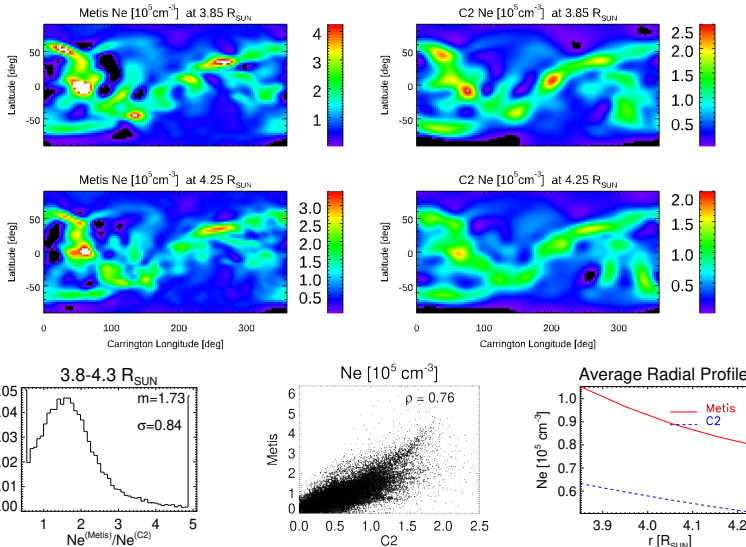
Sequence No.	Date range	Interval [days]	$D_{\text{SUN}}$ [AU]	Lat [deg]	$\Delta\text{Lon}$ [deg]	FoV [ $R_{\odot}$ ]
<b>Meris:</b>						
1	Sep. 03 to 17	13.2	0.73 to 0.57	-3.1 to -5.4	166.5	4.5 – 6.0
2	Sep. 14 to 29	14.4	0.62 to 0.42	-5.0 to -7.7	167.6	3.8 – 4.3
3	Nov. 09 to 23	13.3	0.59 to 0.74	+7.9 to +7.2	168.5	4.8 – 6.0
<b>C2:</b>						
1	Sep. 03 to 16	13.0	1.00 to 1.00	+7.2 to +7.2	178.0	2.3 – 6.3
2	Sep. 14 to 27	13.0	1.00 to 0.99	+7.2 to +6.9	171.6	2.3 – 6.3
3	Nov. 09 to 22	12.8	0.98 to 0.98	+3.5 to +2.0	168.1	2.2 – 6.2

# Segment-1: Metis and C2 Reconstructions of $N_e$



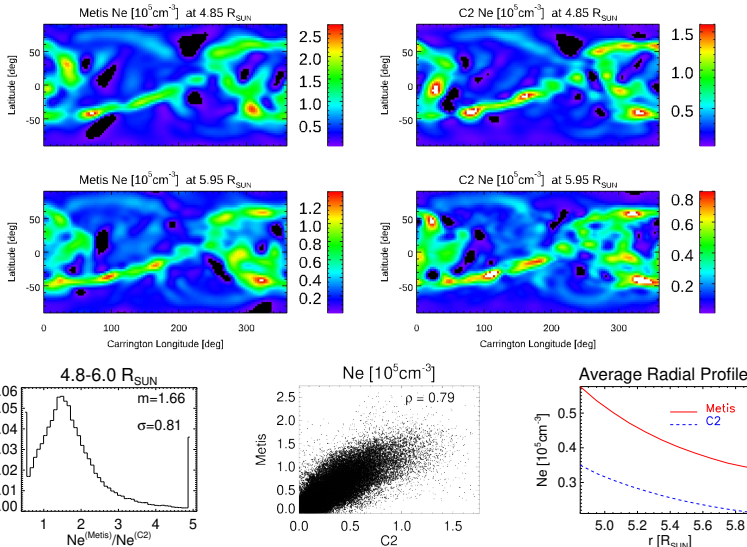
$$\text{Median} \left( N_e^{(\text{Metis})} / N_e^{(\text{C2})} \right) \approx 1.73$$

## Segment-2: Metis and C2 Reconstructions of $N_e$



$$\text{Median} \left( N_e^{(\text{Metis})} / N_e^{(\text{C2})} \right) \approx 1.73$$

# Segment-3: Metis and C2 Reconstructions of $N_e$

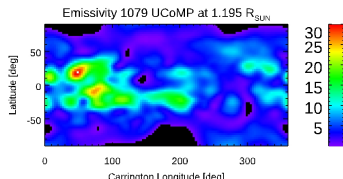
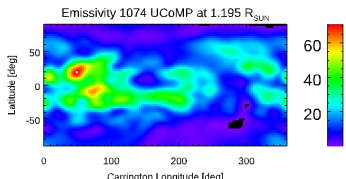
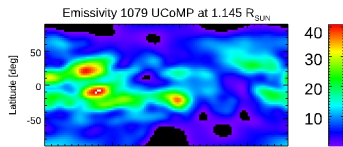
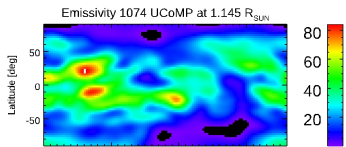
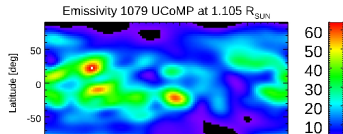
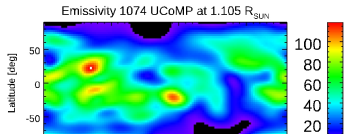
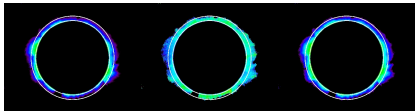
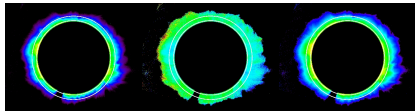


$$\text{Median} \left( N_e^{(\text{Metis})}/N_e^{(\text{C2})} \right) \approx 1.66$$

## Comments on Metis versus C2

- The Metis FoV varies from  $\approx 5.8 - 10.2 R_{\odot}$  at its maximum aphelion  $\approx 1$  AU, down to  $\approx 1.7 - 3.0 R_{\odot}$  at its minimum perihelion  $\approx 0.28$  AU, nearly always overlapping significantly the C2 FoV ( $\approx 2.5 - 6.0 R_{\odot}$ ).
- Comparison of Metis and C2 WL images:  $\text{Median} \left( pB^{(\text{Metis})} / pB^{(\text{C2})} \right) \approx 1.6$ .
- Comparison of Metis or C2 tomography:  $\text{Median} \left( N_e^{(\text{Metis})} / N_e^{(\text{C2})} \right) \approx 1.7$ .
- The systematic discrepancy is not due to lack of perfect opposition and/or simultaneity, nor different distances to Sun, but to calibration procedures. A thorough comparison analysis is under way ([Burtovoi et al. 2024](#)).
- Tomography may aid instrumental intercalibration: while the images obtained by an instrument greatly depend on its location, the reconstructed density does not.
- This research was recently submitted to *Solar Physics* ([Vasquez et al. 2024 a,b](#)).

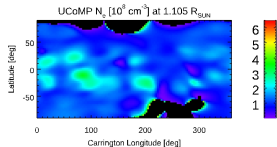
# SRT with UCoMP 1074 & 1079: 3D Emissivity



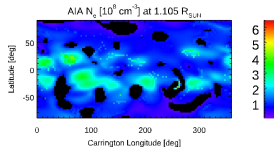
# 3D-Density Reconstruction with Three Diagnostics

September 2022 Simultaneous Tomography with three different instruments

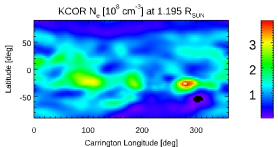
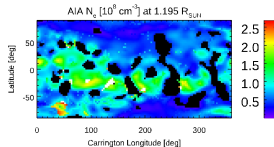
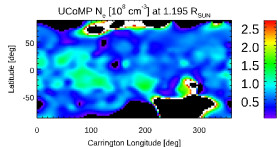
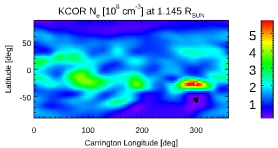
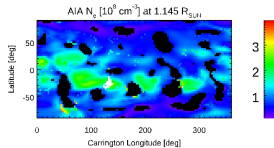
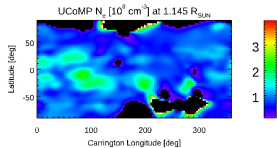
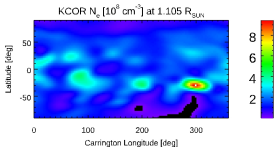
UCoMP 1074/1079



SRT-AIA

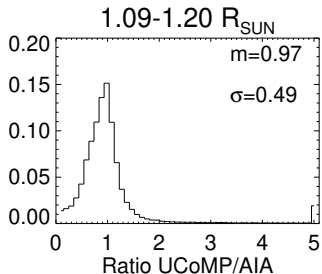


SRT-KCOR

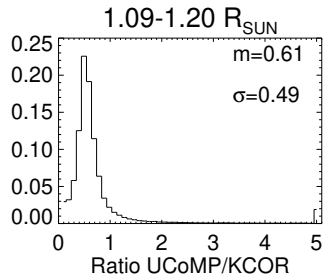


# Comparison of Reconstructed Density

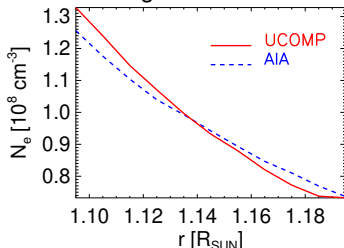
UCoMP versus AIA



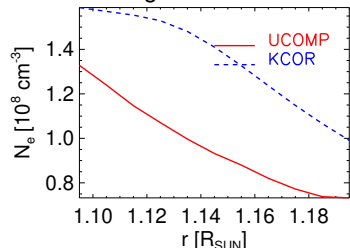
UCoMP versus KCOR



Average Radial Profiles



Average Radial Profiles



# Comments on UCoMP versus AIA versus KCOR

- Emission lines to which UCoMP and AIA are sensitive are produced by Fe ions.
- The UCoMP-SRT  $N_e$  is independent of [Fe], while SRT-AIA  $N_e \propto 1/\sqrt{[Fe]}$ . Comparison of their reconstructed  $N_e$  can in principle provide constraints on the 3D distribution of [Fe], as well as the coronal filling factor affecting emission lines.
- The significantly larger SRT-KCOR  $N_e$  compared to SRT-AIA  $N_e$  has been consistently found for other periods ([Lloveras et al. 2019](#)). Discrepancy can be due to calibration issues, coronal [Fe], and/or coronal filling factor.

# Final Remarks

- As new coronagraphs becomes available, opportunities for development and application of SRT arise.
- Metis simultaneously records WL and Lyman- $\alpha$ . Their combined SRT products can provide 3D constraints on the wind speed. The concept was probed with synthetic images from 3D-MHD simulations of the solar corona (see [Poster](#)).
- UCoMP images expand SRT 3D diagnostics. Multi-instrument tomography with:
  - [SDO/AIA](#) → 3D filter band emissivity in 1 – 4 MK EUV bands.
  - [MLSO/KCOR](#) → 3D  $N_e$ .
  - [MLSO/UCoMP](#) → 3D emissivity in 1 – 3 MK visible Fe lines.

Joint analysis of all SRT products over common FoV  $\approx 1.1 - 1.2 R_\odot \rightarrow$   
3D  $N_e, T_e, \sigma_N, \sigma_T, [\text{Fe}]$ .

---

Thanks so much for having me!